Membrane/water partitioning and permeabilities of perfluoroalkyl acids and four of their alternatives and the effects on toxicokinetic behavior

Andrea Ebert[1,2,☯] * and Flora Allendorf[1☯], Urs Berger[3], Kai-Uwe Goss[1,4], and Nadin Ulrich[1]

[1] Department of Analytical Environmental Chemistry, Helmholtz Centre for Environmental Research - UFZ, Permoserstrasse 15, D-04318 Leipzig, Germany

[2] Institute of Biophysics, Johannes Kepler University, Gruberstrasse 40, 4020 Linz, Austria

[3] Department of Analytical Chemistry, Helmholtz Centre for Environmental Research - UFZ, Permoserstrasse 15, D-04318 Leipzig, Germany

[4] Institute of Chemistry, University of Halle-Wittenberg, Kurt-Mothes-Strasse 2, D-06120 Halle, Germany

* Corresponding author: andrea.ebert@ufz.de

☯ These authors contributed equally to this work.

Abstract

The search for alternatives to bioaccumulative perfluoroalkyl acids (PFAAs) is ongoing. New, still highly fluorinated alternatives are produced in hopes of reducing bioaccumulation. To better estimate this bioaccumulative behavior, we performed dialysis experiments and determined membrane/water partition coefficients, $K_{mem/w}$, of six perfluoroalkyl carboxylic acids (PFCAs), three perfluoroalkane sulfonic acids and four alternatives. We also investigated how passive permeation might influence the uptake kinetics into cells, measuring the passive anionic membrane permeability P_{ion} through planar lipid bilayers for six PFAAs and three alternatives. Experimental $K_{mem/w}$ and P_{ion} were both predicted well by the COSMO-RS theory (logRMSE 0.61 and 0.46, respectively). $K_{mem/w}$ were consistent with literature data, and alternatives showed similar sorption behavior as PFAAs. Experimental P_{ion} were high enough to explain observed cellular uptake by passive diffusion with no need to postulate the existence of active uptake processes. However, predicted pK_a and neutral permeabilities suggest that also the permeation of the neutral species should be significant in case of PFCAs. This can have direct consequences on the steady-state distribution of PFAAs across cell membranes, and thus toxicity. Consequently, we propose a model to predict pH-dependent baseline toxicity based on $K_{mem/w}$, which considers the permeation of both neutral and anionic species.

33 **Introduction**

34 Long-chain perfluoroalkyl acids (PFAAs) including perfluoroalkyl carboxylic acids (PFCAs, e.g.
35 perfluorooctanoic acid PFOA) and perfluoroalkane sulfonic acids (PFSAs, e.g. perfluorooctanesulfonic acid
36 PFOS) have long been in the focus of scientific research due to their persistent and bioaccumulative
37 nature.[1, 2]PFAAs have been produced for seven decades and widely used as processing aids in
38 fluoropolymer production, as components in aqueous film forming fire fighting foams, or as mist
39 suppressants in the chromium plating industry, amongst other applications.[2] Additionally, a wide range of
40 highly fluorinated substances have been and are still used in surface treatment of textiles, leather, paper
41 and board. Many of these highly fluorinated substances can degrade in the environment to form PFAAs.[3]
42 Today, PFAAs are ubiquitously present in the environment and can be found in organisms, including
43 humans.[4-6] Regulatory or voluntary production restrictions for long-chain PFAAs (PFCAs ≥ C8; PFSAs ≥ C6)
44 in the early 2000s led to a shift in production to short-chain PFAAs and alternative compounds.[7-11] The
45 latter include structurally similar poly-fluorinated compounds that are often ether-based (our selected
46 alternatives are shown in Figure S1.1 in the Supporting Information SI).[12]

47 There is growing evidence that also alternatives to the classical PFAAs bioaccumulate.[13] Often the
48 partitioning of a compound between octanol as an organic phase and water has been used to estimate the
49 bioaccumulative potency of that compound.[14-17] In case of ions the octanol/water partition coefficients do
50 not show a correlation to the sorption behavior to biological matrices[14] and should therefore not be used
51 as a surrogate.

52 Monitoring data revealed that PFAAs can mainly be found in liver and blood, but not in adipose tissue.[18-
53 21] It was suggested that especially protein-rich and phospholipid-rich tissues have high sorption capacities
54 for these compounds.[22-26] Indeed, PFAAs were found to sorb strongly to serum albumin[24, 27-31], alpha
55 globulins[25, 32] and fatty acid-binding proteins.[23, 33, 34] Moreover, several studies report binding of PFAAs to
56 phospholipids (Figure S1.2), the major component of biomembranes.[35-43] Phospholipid/water partition

57 coefficients were shown to be an appropriate surrogate for biomembrane/water partition coefficients –
58 for the neutral and ionic species.[44] For uniformity, we will refer to both partition coefficients as
59 membrane/water partition coefficients $K_{mem/w}$.

60 Moreover, $K_{mem/w}$ can be used to assess the nominal compound concentration at which baseline toxicity
61 (narcosis) occurs. This effect is not caused by specific compound-cell interactions but by the accumulation
62 of a compound in the lipid bilayer. When a compound reaches a lipid concentration of about
63 200 mmol/kg_{mem}, it disrupts the proper functioning of the membrane.[45] Both ionic and neutral species of
64 a compound may partition into the membrane and thus contribute to this toxic effect. Due to a pH-
65 gradient over the membrane, there may also be an accumulation of the freely dissolved compound inside
66 the cell. This so-called ion-trapping effect may increase the total internal concentration of the compound,
67 in extreme cases by several orders of magnitude.[46]

68 For PFAAs not much is known about how they enter the cell. Potential transport mechanisms are either
69 active transport (energy consuming), facilitated transport (not investigated here) or passive diffusion
70 (along a gradient across a membrane, defined as passive permeation). Currently, active transport of PFAAs
71 is usually deemed responsible for the absorption process. [47, 48] Passive diffusion as another possibility for
72 transport is often not considered because it is simply assumed that only the neutral species can permeate
73 across membranes.[49] The acidic groups of PFAAs are more than 99.999% dissociated at physiological pH
74 due to their very low pK_a (<1)[50, 51] and should – according to this assumption – not pass the membrane
75 barrier passively. Moreover, several studies reported membrane proteins that actively transport PFAAs.
76 These transporters are located in tissue epithelia involved in reabsorption of PFAAs such as the kidney,[52-
77 57] liver[58-61] and intestine[59]. The studies aimed to explain gender- and species-specific pharmacokinetics
78 observed for PFAAs[52, 62] and seem to confirm that the transport of this compound class is managed by
79 energy-consuming proteins. However, for several hydrophobic anions including permanent ions, it was

80 shown that the anionic fraction can permeate the membrane by passive diffusion.[63, 64] Thus, passive
81 permeation could potentially be a significant or even the dominating pathway also for PFAAs.

82 Respective studies that focused on active transport investigated specialized epithelia proteins. They
83 conducted their experiments with isolated hepatocytes[58, 60, 61] or cell-lines that were genetically modified
84 to over-express the investigated transport protein.[53-56, 59] From these *in vitro* observations it cannot be
85 concluded that membrane proteins are responsible for most of the PFAA transport in an organism. In an
86 *in vivo* situation one has to consider that a PFAA molecule has to pass membrane barriers consisting of not
87 one but many various epithelia types and several epithelia layers and that different membrane tissues
88 express their transport proteins to different extents. The same studies reporting active transport of PFAAs
89 show that passive transport of these compounds is actually occurring: To determine the net uptake of
90 PFAAs, cells which expressed the transport protein were compared to controls – cells that lack this
91 transporter. In all studies an uptake was observed in the controls.[53-55, 58-61] For these controls the measured
92 uptake of the investigated PFAAs should be solely the result of passive diffusion across the cell membrane.
93 It is not clear whether this passive diffusion is dominated by the small neutral fraction of PFAAs or by the
94 high anionic fraction that would cross the membrane less readily due to its charge. This, however, would
95 have direct implications on how the ion-trapping effect and thus baseline toxicity will respond to pH
96 changes outside the cell.

97 To address all these questions, we determined $K_{mem/w}$ for a series of PFAAs and the four alternatives by
98 dialysis experiments. Further, anionic permeabilities for six PFAAs and three alternatives were measured
99 with planar lipid bilayer membranes. All experimentally determined data were compared to predicted
100 values and literature data and used to calculate the external concentration that can initiate baseline
101 toxicity for varying external pH values.

102

103 **Materials and Methods**

104 Chemicals

105 PFAAs and alternatives examined here: perfluorobutanoic acid (PFBA), perfluorohexanoic acid (PFHxA),
106 perfluoroheptanoic acid (PFHpA), perfluorooctanoic acid (PFOA), perfluorononanoic acid (PFNA),
107 perfluorodecanoic acid (PFDA), perfluoroundecanoic acid (PFUnDA), perfluorododecanoic acid (PFDoDA),
108 perfluorobutane sulfonic acid (PFBS), perfluorohexane sulfonic acid (PFHxS), perfluorooctane sulfonic acid
109 (PFOS), dodecafluoro-3H-4,8-dioxanonanoate (DONA), 2,3,3,3-tetrafluoro-2-(1,1,2,2,3,3,3-
110 heptafluoropropoxy-)propanoic acid (HFPO-DA), 9-chlorohexadecafluoro-3-oxanonane-1-sulfonate (9Cl-
111 PF3ONS), perfluoro-4-ethylcyclohexanesulfonate (PFECHS).

112 All other used chemicals, their abbreviations and suppliers are stated in the Supporting Information (SI)
113 section S2.1.

114

115 Preparation of liposomes

116 Liposomes composed of POPC (1-palmitoyl-2-oleoyl-glycero-3-phosphocholine) (Figure S1.2) were
117 prepared as described before[65, 66]. POPC was used for the formation of liposomes to allow a direct
118 comparability to results from Bittermann et al..[67] POPC was weighed and dissolved in chloroform. A thin
119 film of the suspension was formed using a rotary evaporator and was dried overnight. Buffer solution
120 (HBSS; pH 7.4, S2.2) was added and multilamellar vesicles were formed under gentle agitation. The
121 suspension was subjected to a freeze-and-thaw cycle (10x) with liquid nitrogen to produce intermediate-
122 sized unilamellar vesicles. The suspension was then extruded tenfold through a polycarbonate membrane
123 with 0.1 µm pore size (Whatman) in a mini-extruder (Avanti Polar Lipids) at room temperature, generating
124 homogeneous POPC-liposomes.[68] Liposome stock solutions were subsequently used for the dialysis

125 experiments. The POPC content was determined indirectly measuring the phosphorus content using ion
126 chromatography (ICS-6000, Thermo Scientific). After addition of potassium persulfate, the solution was
127 incubated at 90°C overnight, according to a protocol by Huang et al.[69] The recovery of the initially weighted
128 POPC was analyzed for each experiment. Recovery ranged from 72 – 120%. The resulting error in the
129 corresponding $K_{mem/w}$ was small compared to the error resulting from the experimental setup and
130 quantification (which is in the range of ± 0.2 log units).[70]

131

132

133 Dialysis Experiments

134 Individual methanol stock solutions of PFAAs and alternatives were diluted in HBSS (≈20 µg/L) and samples
135 of these dilutions were quantified to determine the exact concentration. Dialysis cells were used as
136 described before.[27, 68, 71] (Figure S2.3) They were composed of two glass chambers separated by a cellulose
137 membrane which was impermeable to liposomes (Por 4, molecular cut-off 12 – 14 kDa, Spectrum
138 Laboratories Inc.). Test and reference cells were prepared for each compound in triplicates. The latter
139 were used to check for equilibrium between the two chambers and for determining the freely dissolved
140 analyte mass in total (mass balance was applied due to loss of compounds by adsorption on the glass
141 surface, see calculations below). For the test cells, liposome stock solutions were added to the buffer
142 solution in one chamber to the final volume of 5 mL, while for the reference cells, this chamber contained
143 only buffer solution. In both, test and reference cells, 5 mL analyte buffer solution were added into the
144 second chamber. Dialysis cells were incubated at 310 K in darkness, the solutions in each chamber were
145 stirred at 470 rpm. When equilibrium was reached, the liposome-free chamber of the test cells and both
146 chambers of the reference cells were sampled. For each compound, the fraction sorbed to the liposomes
147 was kept between 20 – 80 % to reduce measuring uncertainty (S2.4). To this end, the concentration of

148 POPC in solution was adapted with respect to the sorption behavior of the investigated compound and
149 ranged from 0.0025 to 2 g/L (based on chamber volume of 5 mL). The molar ratio between the compound
150 sorbed and the total amount of phospholipids was held below 0.08 which is assumed to be within the
151 linear range of the sorption isotherm.[67, 68]

152

153 Instrumental analysis

154 Quantification of all samples was done by ultra performance liquid chromatography with tandem mass
155 spectrometry (UPLC-MS/MS; Xevo TQ-S Waters Corporation) in negative electrospray ionization mode (for
156 detailed description see S2.5 and references[27, 72, 73]).

157 Calculation of membrane/water partition coefficients $K_{mem/w}$

158 The membrane/water partition coefficient $K_{mem/w}$ in L_w/kg_{mem} was calculated with

159 $$K_{i,mem/w} = \frac{c_{i,mem*}}{c_{i,w*}} \quad (1)$$

160 where i refers to the analyte and *states the equilibrium condition. $c_{i,mem}$ is the bound concentration to
161 the membrane (g/kg_{mem}) and $c_{i,w}$ is the concentration in water (g/L_w). The latter was quantified directly
162 from the test cells. Following the mass balance, the mass of analyte which was bound to the membrane
163 $m_{i,mem}$ was deducted by subtracting the determined mass of analyte which was freely dissolved in the
164 buffer solution($m_{i,free}$) from the total analyte mass in the dialysis system ($m_{i,total}$) in equilibrium.

165 $$m_{i,mem} = m_{i,total} - m_{i,free} \quad (2)$$

166 Certain poly- and perfluorinated compounds adsorbed to a different extent to the glass surface of the
167 custommade, not exactly identically shaped chambers. For all compounds reference cells that contained
168 no liposomes were taken for the determination of $m_{i,total}$. For compounds that adsorbed substantially

169 (>10%) to the glass surface such as long-chain PFUnDA, PFOS and 9Cl-PF3ONS, an extraction step with
170 methanol for the individual dialysis cells (test cells) was performed to yield a closed mass balance. The
171 buffer solution was removed for extraction, 2 mL of methanol were added and the dialysis cells were
172 shaken for one hour. The methanol extracts were analyzed and $m_{i,mem}$ was calculated taking into account
173 the loss due to adsorption. Considering these adsorption effects, total recoveries varied between 92 –
174 110%. For determination of $K_{mem/w}$, mean and standard deviation of six measurements (three
175 measurements on each of two days) were taken.

176

177

178

179 Formation of planar lipid bilayers

180 For the anionic membrane permeability measurements, solvent depleted membranes were formed from
181 DPhPC (1,2-diphytanoyl-sn-glycero-3-phosphocholine) in hexane (10 mg/mL) using the Montal-Mueller
182 technique[74], as described in Ebert et al. [63] DPhPC was chosen due to its high membrane stability and the
183 direct comparability to results from Ebert et al.. [63] The membrane was folded across a hole (diameter: ~80–
184 150 µm) in a pretreated (0.5% (v/v) hexadecane in hexane) Teflon septum (25 µm thick) separating two
185 compartments of a Teflon chamber filled with buffered solution at pH 7 (1.3 mL each; 100 mM KCl; 5 mM
186 MOPS, S2.1). In each compartment (on opposite bilayer sides) an Ag/AgCl electrode was placed, and
187 membrane formation was assessed by the specific capacity (range: ~0.6–0.8 mF/cm^2). See Figure S2.6 for
188 setup schematics.

189

190 Anionic membrane permeability experiments

191 Voltage was applied to the electrodes placed in both compartments, and the resulting current was
192 measured. Only a charged compound traversing the membrane will lead to an electrical signal. This

193 method allows measuring the permeability of ionic compounds across the membrane, even if the neutral
194 effective permeability (permeability*fraction of neutral species) is greater than the ionic permeability,
195 meaning even if the flux following a chemical gradient is dominated by the neutral species.
196 After membrane formation, control curves without any compound addition were measured. The
197 respective compound to be examined was added in equal amounts on both sides of the membrane (no
198 chemical gradient) using concentrated stock solutions dissolved in either water or DMSO. In case DMSO
199 was used, the DMSO concentration did not exceed 1%. The buffer solution was well stirred by magnetic
200 bars to allow for a rapid mixing after addition of the chemical. All measurements were performed at room
201 temperature. Data were recorded using the HEKA EPC10 patch clamp amplifier (HEKA Elektronik Dr.
202 Schulze).
203 Each compound was measured on at least three different membranes. Multiple ramp voltage sweeps
204 (from -100 to 100 mV) per added chemical concentration were conducted to measure the steady-state
205 electrical membrane conductance. The resulting current/voltage characteristics were evaluated as
206 described in detail in Ebert et al.[63]. In short, the anionic permeability P_{ion} was derived from the specific
207 conductance G_s (G divided by membrane area) using the Goldman-Hodgkin-Katz flux equation in absence
208 of a chemical gradient:

$$P_{ion} = \frac{R * T}{z^2 * F^2} * \frac{G_s}{c} \tag{3}$$

209

210 with R being the gas constant, T the temperature in Kelvin, z the valence of the ion, F the Faraday constant
211 and c the freely dissolved ion concentration. The chambers were tested against adsorption effects and,
212 due to their low pK_a, at pH 7 all examined compounds were near 100% dissociated. Thus the freely
213 dissolved anionic concentration was assumed to be equal to the added total concentration of the
214 respective compound. The only exception was PFDoDA, which adsorbed about 50-80% to our Teflon

215 chambers. In that case only the freely dissolved concentration was considered to calculate membrane
216 permeability.
217
218 Predictions of permeabilities, partition coefficients and pK_a
219 If no or only partial experimental data were available, predictive methods already established in the
220 literature were used to generate missing parameters, such as pK_a or neutral permeability P_n. Additionally,
221 our experimental results for $K_{mem/w}$ and P_{ion} were compared to these predictions, to assess their predictive
222 power for PFAAs.

223 Membrane permeability P and $K_{mem/w}$ for both the neutral and the anionic species were predicted using
224 the software COSMOtherm[75] (Dassault Systèmes Deutschland GmbH) or its integrated tools
225 COSMOmic/COSMOperm. We also chose this software to predict neutral permeability P_n. Other predictive
226 methods[76] are not applicable for ions and may depend on a structural similarity between their training
227 dataset and the compounds to be predicted, while COSMOtherm/COSMOperm is an ab initio approach. It
228 uses quantum chemically optimized structures of molecules (so called COSMOfiles, generated with
229 Turbomole[77]). To account for the fact that different conformers of a compound may be energetically
230 favourable in different solvents, COSMOconf (V. 4.1;[78]) was used to create various relevant conformers.
231 COSMOtherm itself is based on the COSMO-RS (Conductor-like Screening Model for Realistic Solvation,[79])
232 theory which uses physical intermolecular interactions (e.g. electrostatic, hydrogen bonding and van der
233 Waals interactions) to predict e.g. partition coefficients or pK_a values.
234 For the prediction of $K_{mem/w}$ by COSMOmic or P by COSMOperm, membrane anisotropy is considered by
235 dividing the membrane in 60 different homogeneous layers (derived from molecular dynamics
236 simulations). Then, layer specific partition coefficients are calculated. The minima of the resulting energy
237 profile (the positions with a high compound probability) determine $K_{mem/w}$, while the energy maxima
238 (lowest compound probability) represent the main barrier for P.

239 The applied methods to predict *P* are based on the solubility-diffusion model, which assumes that the
240 permeability depends on the partition into and diffusion through the membrane. Implying that the main
241 barrier for membrane transport lies in the membrane centre, these calculations can be simplified:
242 Hexadecane can be used as a surrogate for the inner hydrocarbon part of the membrane and the
243 calculations of *P* can be based on the partitioning from water into hexadecane. [63, 80] Details on the used
244 methods and the used parametrizations are stated in Table S2.7. The pK_a values were predicted using
245 either the predictive tool COSMOtherm or the software JCHEM for Office (ChemAxon).[81]
246
247 Baseline toxicity and ion-trapping
248 Baseline toxicity is believed to be caused by the disturbance of membrane functioning due to the presence
249 of compounds in the membrane (at a concentration exceeding ~200 mmol/kg_{mem})[45]. The freely dissolved
250 concentration in water c_w outside that membrane that corresponds (in a thermodynamic equilibrium
251 situation) to this threshold depends on the membrane/water partition coefficient $K_{mem/w}$ (see S2-8 for
252 detailed derivations):
253

$$c_w = \frac{200\ mmol/kg_{mem}}{K_{mem/w}} \tag{4}$$

254

255 If we assume partitioning into the outer membrane of the cells as the cause of baseline toxicity (neglecting
256 any possible ion-trapping effects), this c_w would represent the effective concentration EC_{50} in the exposure
257 solution at which baseline toxicity occurs.[46]

258 Yet, if there was a concentration increase inside the cell due to an ion-trapping effect, or if the partitioning
259 into the membrane of a specific cell organelle was the cause of baseline toxicity, the freely dissolved
260 concentration in the cytosol (and not in the exposure solution) might determine the toxicity. To calculate

261 the external concentration that corresponds to the respective cytosolic concentration in a steady-state
262 situation, compound fluxes across the outer membrane have to be considered. At steady-state, no net flux
263 occurs, and thus the flux of the neutral species (driven by concentration gradient) and the flux of the
264 anionic species (driven by concentration gradient and electrical potential ΔV) must be equal in size and
265 opposite in direction. The freely dissolved external concentration in water c_{ext} might then be expressed as
266 follows (S2.8):

$$c_{ext} = \frac{\frac{P_n * f_{n,cyt}}{P_{ion}} + f_{ion,cyt} * \frac{zF}{RT}\Delta V \frac{1}{1-\exp(-\frac{zF}{RT}\Delta V)}}{\frac{P_n * f_{n,ext}}{P_{ion}} + f_{ion,ext} * \frac{zF}{RT}\Delta V \frac{\exp(-\frac{zF}{RT}\Delta V)}{1-\exp(-\frac{zF}{RT}\Delta V)}} * \frac{200\ mmol/kg_{mem}}{K_{mem/w}} \quad (5)$$

267 Where z is the valence of the ion (-1), F is the Faraday constant, R the gas constant, and T the temperature
268 in K (295 K), $f_{n,ext}$ and $f_{n,cyt}$ the neutral fractions and $f_{ion,ext}$ and $f_{ion,cyt}$ the anionic fractions outside the cell or
269 inside the cytosol respectively. In case of ion-trapping, c_{ext} would represent the effective concentration
270 EC_{50} outside the cell that would lead to a concentration of 200 mmol/kg_{lipid} inside the membrane, and thus
271 to baseline toxicity.

272 **Results and Discussion**

273 Membrane/water partition coefficients

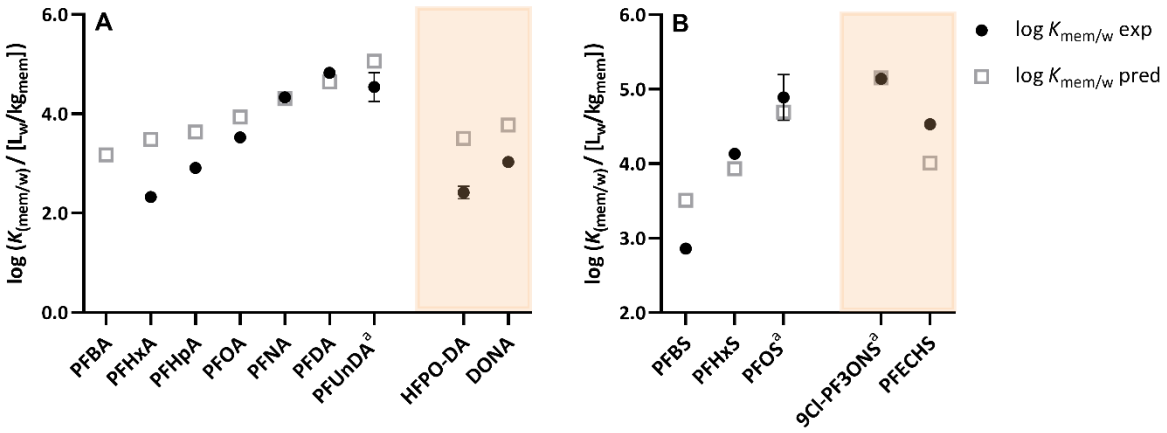

274

275 **Figure 1.** Logarithmic experimental membrane/water partition coefficient $K_{mem/w}$ of six PFCAs and two alternatives
276 with carboxylic acid groups HFPO-DA and DONA (A). Log $K_{mem/w}$ exp of three PFSAs and two alternatives with sulfonic
277 acid groups 9Cl-PF3ONS and PFECHS (B). For comparison, log $K_{mem/w}$ predicted from COSMOmic are also given (empty
278 squares). Error bars representing standard deviations (three measurements on each of two days) are partly covered
279 by symbols of data points. For all compounds marked with a, an extraction step was included because of high
280 adsorption to glass surfaces.

281 Results of the equilibrium dialysis experiments are shown in Figure 1 and listed in Table S3.1.1-3.1.2.
282 Experimental $K_{mem/w}$ of PFAAs and alternatives ranged from 2.3 to 5.1 log units. It can be seen that for both
283 PFCAs and PFSAs, $K_{mem/w}$ increase with increasing chain length, because more surface area for van der
284 Waals interaction becomes available.[82] The incremental increase in $K_{mem/w}$ per perfluorinated carbon is
285 about the same for PFCAs and PFSAs (global fit: 0.63 log units / carbon, single fits 0.63/0.61 respectively;
286 see Figure S3.1.3 for details). According to the intercepts of the fit, PFSAs sorb in general about 1.2 log
287 units more strongly to the membrane than PFCAs with the same number of perfluorinated carbons.

288 PFUnDA is the only outlier to this trend. A deviation from linearity in $K_{mem/w}$ with increasing number of
289 carbon atoms in the side-chain was reported in literature for 1-alkyl-3-methylimidazolium derivatives.[83]
290 The so called "cut-off effect" was supposedly caused by a reduced diffusibility due to the size and flexibility
291 of the longer alkyl side-chains. Yet, our experimental uncertainty for PFUnDA allows no direct conclusion
292 whether the decreased Kmem/w is a consequence of the "cut-off effect".. Long-chain compounds such as
293 PFUnDA and PFOS show relatively high standard deviations. More than 10% of PFOS and more than 70%
294 of PFUnDA was adsorbed to the glass surface during the dialysis experiment (Table S3.1.2). An additional
295 extraction step needed to be performed, increasing the error in the determination of $K_{mem/w}$, and also
296 limiting the compounds that could be analyzed with our setup. PFUnDA is therefore the highest PFCA
297 analogue for which $K_{mem/w}$ was determined.

298 For PFBA as the shortest investigated PFCA homologue, the $K_{mem/w}$ was lower than what could be
299 experimentally determined (<1.7 log units), because the manually operated extruder for preparing the
300 liposomes could not be used for higher concentrations than 10 g/L POPC due to the resulting higher
301 pressure. The lipid concentration could not be increased any further, since the fraction bound would drop
302 below 20%, in turn increasing the measuring uncertainty (S2.4).

303 The two alternatives with carboxylic groups, HFPO-DA and DONA display log $K_{mem/w}$ of 2.4 and 3.0,
304 respectively and are thus in the range of the classical PFAAs (HFPO-DA comparable to PFHxA; DONA
305 comparable to PFHpA). Neither the incorporated ether groups nor the non-perfluorinated carbon atom
306 next to the ether group in DONA or the side-chain in HFPO-DA seem to significantly affect the sorption
307 behavior to membranes. We made similar observations for the two alternatives when investigating the
308 sorption to serum albumin in an earlier study.[27] We attribute this effect to the chemical structure of the
309 compounds, as can be visualized by the sigma surfaces of COSMOconf/TURBOMOLE software (S3.1.4). The
310 high electron negativity of neighboring fluorine atoms decreases the electron donor ability of the oxygen

311 (-CF_2-O-CF_2- group). This will lower the polarity of an ether group linked to fluorinated carbons and could
312 explain why the sorption strength of these alternatives is not affected by the incorporated oxygen.[27]

313 The two sulfonates 9Cl-PF3ONS and PFECHS have eight perfluorinated carbons, like PFOS. The $K_{mem/w}$
314 values of 5.1, 4.5 , and 4.9 log units, respectively, do not show strong differences. We thus conclude that
315 all alternatives examined in this study did show a very similar sorption behavior to the membrane as the
316 classical PFAAs.

317 Predicted membrane/water partition coefficients

318 With a logRMSE of 0.61 the predicted values corresponded well to our experimental data (Fig. 1 and Table
319 S3.1.1) and were well within the general prediction accuracy of COMOmic for ions of RMSE=0.7 log units.[67]
320 However, there is a systematic overprediction for small $K_{mem/w}$ (<4 log units), since the plot of predicted
321 $K_{mem/w}$ against the number of perfluorinated carbons shows a systematically shallower slope, as compared
322 to experimental values (Figure S3.1.3.).

323

324 Membrane/water partition coefficients of PFAAs in literature

325 When compared to our experimental results for $K_{mem/w}$, all values reported in a study by Droge[43] matched
326 our data within the boundaries of the typical experimental error of 0.2 log units (Figure S3.1.5). The
327 comparison comprises our complete series of PFAAs except for PFUnDA. Several other studies have
328 described the sorption of one or more PFAAs to the membrane determined with various methods.[35-43]
329 From most of these methods only qualitative trends were derived by measuring and comparing a series of
330 PFAAs. In accordance with our results these studies show that the sorption of PFAAs to the membrane is

331 increasing with increasing number of perfluorinated carbons/chain-length[41-43] and that PFSAs sorb
332 stronger to the membrane than PFCAs[40-43].

333

334 Permeabilities of PFAAs and alternatives

335 Anionic permeabilities were measured for three PFCAs, three PFSAs, and three alternatives in DPhPC
336 bilayer membranes. Results of the anionic permeability measurements are shown in Figure 2 and stated
337 in Table S3.2.1. Measured permeabilities range from $2*10^{-7}$ cm/s to $8*10^{-5}$ cm/s. These values are
338 comparable in their magnitude to very potent uncouplers of phosphorylation, such as 2,4-dinitrophenol
339 (P_{exp}= $3*10^{-7}$ cm/s) or dinoterb (P_{exp}=$1*10^{-4}$ cm/s),[63] which are known for their relatively high anionic
340 permeability.[84]

341 Similar to $K_{mem/w}$, permeability values increase with increasing number of perfluorinated carbons, and
342 PFSAs show higher permeabilities than their carboxylic counterparts. The increased permeability of the
343 PFSAs is probably a consequence of a broader charge distribution in the sulfonate head-group, and thus
344 lower surface charge densities (see Figures S3.2.2 - S3.2.3 for the sigma profiles and sigma surfaces of
345 PFNA and PFOS, quantum chemical calculations).

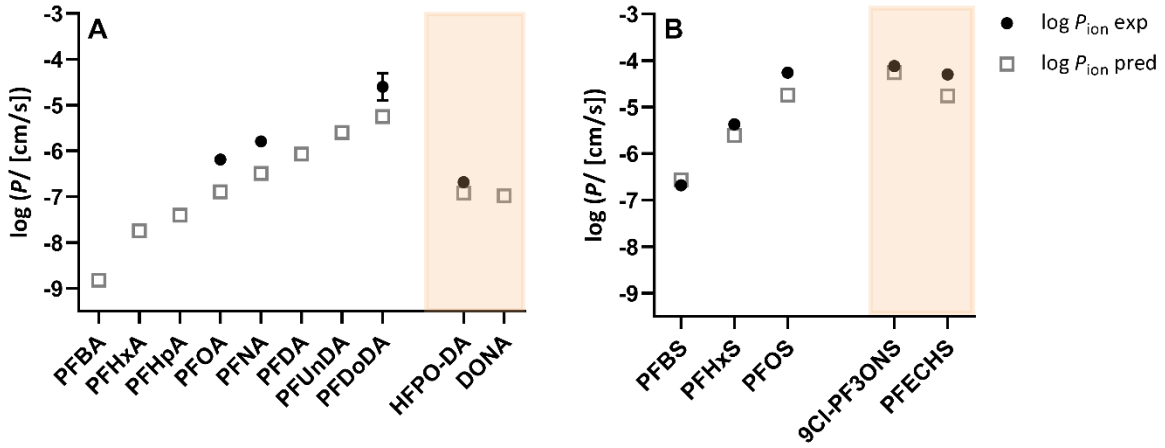

346

347 **Figure 2.** Logarithmic experimental anionic permeabilities P_{ion} of three PFCAs and one alternative with a carboxylic
348 acid group HFPO-DA (A). Logarithmic anionic experimental permeabilities of three PFSAs and the two sulfonic acid
349 alternatives 9Cl-PF3ONS and PFECHS (B). For comparison, anion permeabilities predicted from the hexadecane/water
350 partition coefficient are also given (empty squares). The order of PFCAs/PFSAs corresponds to an increasing chain-
351 length with increasing number of perfluorinated carbons. Permeabilities were measured for each compound with at
352 least three different membranes. The error bars for PFDoDA depict the range of *P* around the logarithmic mean.
353 Higher uncertainty for PFDoDA is the result of stronger and variable sorption to the measurement chamber.

354

355

356 <u>Predicted permeability data</u>

357 Predicted anionic permeabilities (stated in Table S3.2.1) correspond well to the experimental values, as
358 can be seen in Figure 2 and Figure S3.2.4. Predictions were made using either the correlation to the
359 hexadecane/water partition coefficient $K_{hd/w}$ (logRMSE: 0.46) or COSMOperm (logRMSE: 0.88).
360 Permeabilities for PFCAs are slightly underestimated, but the rate of increase of P_{ion} with the number of
361 perfluorinated carbons is roughly the same in experiment and prediction from $K_{hd/w}$. Additionally, we
362 predicted the permeability of the neutral species, again using either a calculation based on $K_{hd/w}$ or
363 COSMOperm respectively (See Methods for more details).

364 To address the question whether neutral or anionic permeability would be the dominating permeation
365 pathway in passive diffusion, ionic permeability was compared to the effective neutral permeability
366 (P_n * f_n= neutral permeability weighed with the fraction of the neutral species that is present at actual pH)
367 at pH 7.4. In contrast to the predictions for the anionic species, predicted P_n are less reliable. They have
368 not been verified and differ between prediction methods (Table S3.2.1). Regardless of the prediction
369 method used for P_n, the same pattern arises though: For all PFCAs and their alternatives, despite their low
370 neutral fraction at physiologic pH, effective neutral permeability (P_n * f_n) is still calculated higher than
371 anionic permeability (see Table S3.2.5). In contrast, for all PFSAs and their alternatives, anionic
372 permeability is orders of magnitude higher than the effective neutral permeability.

373 Consequently, for PFSAs anionic permeation should dominate the permeation process. This should also
374 hold true for lower pH-values, because P_{ion} is orders of magnitude higher than the effective neutral
375 permeability, even when the neutral fraction increases with lower pH. For PFCAs, the dominance is not
376 that clear. Neutral permeabilities through the plasma membrane of Caco-2 cells were suggested to be
377 about 1.8 orders of magnitude lower than through artificial bilayers, likely due to the biomembrane's
378 content in sphingomyelin and cholesterol.[85] Considering such potential differences between
379 biomembranes and artificial bilayer membranes, and uncertainties in the predicted parameters such as
380 pK_a or P_n, permeation dominance may be dependent on pH. It is thus possible that passive permeation of
381 PFCAs may be dominated by the neutral species at low pH, and by the anionic species at high pH.

382

383 <u>Comparison to experimental uptake rates from literature</u>

384 To compare our permeability values for both the anionic and neutral species to the measured uptake rates
385 published in literature, we first converted the data from literature, which were stated in different
386 reference systems, such as uptake per protein weight or per cell number, to a common value of effective

387 permeability P_{eff} [cm/s] (Table S3.2.6). All data from references used here[53, 55, 59-61] had been employed to
388 investigate the relative importance of active transport of PFAAs. The researchers were either able to
389 separate the saturating active transport component and the passive permeation from their uptake rates,
390 or they used empty vectors that were not expressing the examined transport protein in control cells. Thus,
391 the data reflect uptake rates by passive diffusion. Additionally, we calculated the effective permeabilities
392 for the anionic $P_{eff,ion}$ and neutral $P_{eff,n}$ species from our experimental or predicted data (Table S3.2.7).

393 Again, for the PFSAs the available data suggest that their passive uptake into the cell is clearly dominated
394 by the anionic species. We come to this conclusion for the following reasons: (i) The effective anionic
395 permeabilities calculated from the experimental artificial bilayers permeabilities match the effective
396 permeabilities determined from the uptake rates in literature quite well (deviation factor ≤ 3 for all three
397 compounds, Table S3.2.7). (ii) $P_{eff,n}$ are predicted orders of magnitude lower than $P_{eff,ion}$, and can therefore
398 be excluded as the dominant passive permeation pathway. If this reasoning is correct, then P_{eff} should not
399 significantly change with pH. While Zhao et al.[59] did measure also at pH 5.5, they unfortunately did not
400 show the data and only stated that the active transport rate did not significantly change with pH. Whether
401 also the control experiment (with empty vector) was independent of pH, which would support our results,
402 is not stated.

403 For PFCAs, also the comparison to literature seems less distinctive: At pH 7.4, both $P_{eff,ion}$ and $P_{eff,n}$ (and
404 shifted by 1.8 log units to compensate for possible differences between artificial bilayers and
405 biomembranes) are about the same order of magnitude as $P_{eff,lit}$, and could thus both contribute to the
406 effective permeation. From Yang et al.[54], we can see that with increasing pH the uptake rate of PFOA
407 decreases, at pH 7 to 77% of the initial uptake rate at pH 6, at pH 8 to 67% of the initial uptake rate. While
408 this decrease is a sign that neutral permeation should be relevant, because a clearly anionic dominated
409 permeation should show no pH-dependence, the decrease should be much more pronounced if neutral
410 permeability was the dominating species. In that case, the permeation should drop by one order of

411 magnitude for each increase in pH, because the neutral fraction decreases by this factor. Yet, at pH 6, the
412 value predicted for effective neutral PFOA permeation is more than one order of magnitude higher than
413 $P_{eff,lit}$, which indicates that the value might be overestimated. The aforementioned decrease in the uptake
414 rate thus indicates that at pH 6, $P_{eff,ion}$ is higher than $P_{eff,n}$, although $P_{eff,n}$ is still relevant. We would have to
415 decrease our predicted value $P_{eff,n}$ of PFOA by a factor of 300 to be able to reproduce this pH-dependency
416 (see Table S3.2.8).

417 Errors in prediction of pK_a and P_n will directly affect the relation between $P_{eff,ion}$ and $P_{eff,n}$, and not many
418 experimental pH-dependent data are available. Therefore a definite conclusion on the species dominance
419 in the transmembrane transport is not possible. Yet, it seems likely that both species are relevant in the
420 transport process.

421

422

423 Partition and permeability combined: Baseline toxicity

424 To calculate the baseline toxicity of a compound, its partitioning into the membrane, as well as knowledge
425 about the permeability of both the anionic and neutral species are required. As long as the target of
426 baseline toxicity is unclear, both the possibility of external or cytosolic concentration acting on the plasma
427 membrane, or cytosolic concentration acting on the membranes of cell organelles should be considered.
428 While $K_{mem/w}$ is needed to predict the compound concentration adjacent to the membrane that would lead
429 to a toxic effect (Eq. 4), membrane permeabilities across the plasma membrane allow determining which
430 external concentration will lead to the specific cytosolic concentration (via the ion-trapping effect), that
431 will lead to a toxic effect (Eq. 5). Usually, this ion-trapping effect can easily be quantified (Eq. S11), as long
432 as neutral permeation is much larger than the anionic one, which is the case for most compounds. But due

433 to their low pK_a, this is not the case for PFAAs. As discussed above, for PFSAs ionic effective permeability
434 is much larger than neutral effective permeability. As a consequence, we expect concentrations to
435 distribute across the membrane according to the Nernst potential (Eq. S12). With a negative potential
436 inside the cell, this would lead to a concentration decrease of the PFSAs inside the cell, over a large range
437 of different external pH values. For PFCAs, uncertainties in prediction of pK_a and P_n make it difficult to
438 deliver exact predictions: Over the pH range of 5 to 9, we expect permeability of both species to be
439 relevant, and thus we expect toxicity values to change with pH. EC_{50} should lie somewhere in between
440 concentrations resulting from the aforementioned extreme cases of dominating permeation of either
441 species.

442 The toxicity data we found in literature unfortunately did not have a broad range of measured pH, or often
443 the pH value was not stated at all or it changed over time. Even for similar test organisms, the toxicity
444 values at physiologic pH varied widely.[86-88] We thus decided to illustrate the possible implications of the
445 ion-trapping effect with model calculations (Eq. 5). We calculated the EC_{50} for PFOS and PFOA in the
446 external pH-range from 5 to 9, assuming a constant pH of 7.4 inside the cell (Figure 3).Measured anionic
447 permeabilities and the neutral permeabilities predicted from $K_{hd/w}$ (and shifted by 1.8 log units) were used
448 for the calculation. To account for the uncertainties in pK_a and permeability, we systematically varied P_n,
449 up to a factor of 1000. Extreme cases, such as a clear dominance of anionic permeability (orange line) or a
450 clear dominance of neutral permeability (blue line) are marked in Figure 3A,B to illustrate the theoretically
451 possible range of toxic concentrations.

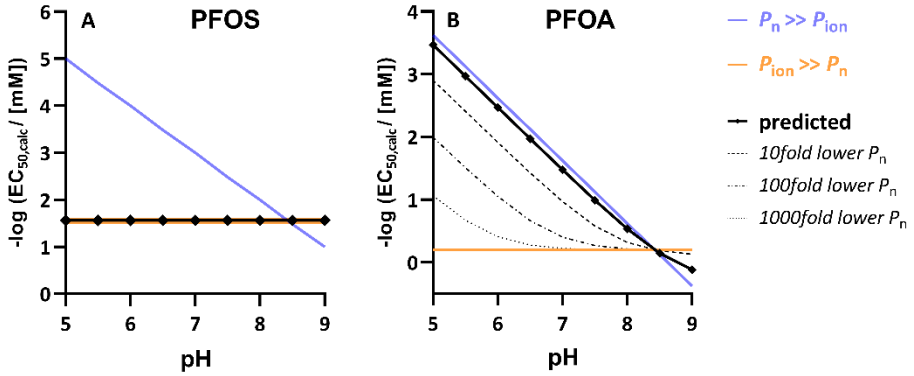

Figure 3. Calculated logarithmic effective concentration EC_{50} for narcosis plotted against the external pH, for PFOS (A) and PFOA (B). Panel (A) and (B) show EC_{50} for extreme cases such as dominating anionic (orange) or neutral (blue) permeabilities The predicted values (black) for PFOS coincide with the extreme case of dominating anionic permeability, while the predicted values for PFOA coincide with the extreme case of dominating neutral permeability. Panel (B) also depicts the results of a sensitivity analysis. If P_n is chosen lower than predicted, the predicted curves stepwise approach the extreme case of dominating anionic permeability.

For PFOS, the predicted values coincide with the extreme case of dominating anionic permeability ($P_{ion} >> P_n$; Figure 3A). The values do thus show no change with pH and are slightly lower than the values calculated without ion-trapping effect, because the compound distributes across the membrane according to the Nernst potential (decreased concentration inside the cell due to negative charge inside). The values were not sensitive at all to a systematic change of the neutral permeability, and the variations are therefore not depicted.

It is not clear whether baseline toxicity acts on the plasma membrane or organelles inside the cytosol. If it acts on the plasma membrane, the calculations without ion-trapping should lead to the most realistic results, because the external concentration would be the relevant one in this case. If it acts on cell organelles, ion-trapping has to be considered, because the concentration in the cytosol would be the relevant one. In contrast, for PFOA, the predicted values almost coincide with the extreme case of dominating neutral permeability ($P_n >> P_{ion}$; Figure 3B). The toxicity thus increases with decreasing external pH, by about one order of magnitude per pH unit. But the result is not as clear as with PFOS, because

471 neither P_n nor P_{ion} clearly dominate permeation if uncertainties in prediction are considered. The sensitivity
472 analysis shows that with decreasing P_n (or alternatively decreasing pK_a, which would result in the same
473 outcome), the pH-dependent increase of toxicity with decreasing pH is less distinct. The predicted values
474 approach the extreme case of dominating anionic permeability, the lower P_n is chosen (dashed curves,
475 Figure 3B).

476 A systemic measurement of toxicity over a broad range of pH values is thus desirable, to assess whether
477 the toxicity of PFCAs at low pH does exceed the one measured at physiologic pH. Such pH-dependent
478 toxicity data are needed, because also in the aquatic environment the pH varies widely.[89] Even if P_n and
479 pH-dependent effects are not considered, the P_{ion} determined in this work seem sufficient to explain
480 observed cellular uptake rates of PFAAs. Compounds with permeabilities higher than $2.5*10^{-7}$ cm/s are
481 absorbed intestinally by more than 10%, and those with permeabilities higher than $6*10^{-6}$ cm/s by about
482 80% according to a correlation between human fraction absorbed and the apparent permeability in Caco-
483 2 cells published by Skolnik et al.[90] So, the anionic permeation alone should lead to a high fraction absorbed
484 in humans for most of the PFAAs including their highly-fluorinated alternatives tested in our work. These
485 alternatives sorbed to the membrane to the same extent as PFAAs, and also their permeabilities did not
486 differ from PFAAs. On their own, these parameters might indicate that the bioaccumulative potency is not
487 lower compared to PFAAs. A study investigating the toxicokinetics of HFPO-DA reported faster elimination
488 compared to PFOA.[91] The discrepancy could be explained by the lower $K_{mem/w}$ of HFPO-DA (similar to
489 PFHxA) as compared to PFOA, and by active transmembrane transport. This does not diminish the
490 importance of passive permeation, since either of the transport processes might dominate permeation,
491 depending on compound concentration[61] or amount and types of transporter proteins in the cell.[52, 60]

492

493 Acknowledgments

The authors thank Heidrun Paschke and Andrea Pfenningsdorff for lab assistance. The presented work contributes to the programme topic Chemicals In The Environment (CITE) funded by the Helmholtz Research Programme.

The authors declare no competing financial interest.

Supporting Information

Details on experimental aspects, prediction methods, derivations of used equations and a complete overview on the used data including graphical display for comparisons and sigma surfaces of several investigated compounds. This information is available free of charge via the Internet at http://pubs.acs.org.

References

1. Conder, J. M.; Hoke, R. A.; Wolf, W. d.; Russell, M. H.; Buck, R. C. Are PFCAs Bioaccumulative? A Critical Review and Comparison with Regulatory Criteria and Persistent Lipophilic Compounds. *Environ. Sci. Technol.* **2008,** *42*, (4), 995-1003.
2. Buck, R. C.; Franklin, J.; Berger, U.; Conder, J. M.; Cousins, I. T.; de Voogt, P.; Jensen, A. A.; Kannan, K.; Mabury, S. A.; van Leeuwen, S. P. Perfluoroalkyl and polyfluoroalkyl substances in the environment: terminology, classification, and origins. *Integr. Environ. Assess. Manag.* **2011,** *7*, (4), 513-41.
3. Lee, H.; D'Eon, J. C.; Mabury, S. A. Biodegradation of Polyfluoroalkyl Phosphates as a Source of Perfluorinated Acids to the Environment. *Environ. Sci. Technol.* **2010,** *44*, (9), 3305-3310.
4. Wang, Z.; Cousins, I. T.; Scheringer, M.; Buck, R. C.; Hungerbühler, K. Global emission inventories for C4-C14 perfluoroalkyl carboxylic acid (PFCA) homologues from 1951 to 2030, Part I: production and emissions from quantifiable sources. *Environ. Int.* **2014,** *70*, 62-75.
5. Houde, M.; Martin, J. W.; Letcher, R. J.; Solomon, K. R.; Muir, D. C. Biological Monitoring of Polyfluoroalkyl Substances: A Review. *Environ. Sci. Technol.* **2006,** *40*, (11), 3463-3473.
6. Ng, C. A.; Hungerbühler, K. Bioaccumulation of perfluorinated alkyl acids: observations and models. *Environ. Sci. Technol.* **2014,** *48*, (9), 4637-4648.
7. Scheringer, M.; Trier, X.; Cousins, I. T.; de Voogt, P.; Fletcher, T.; Wang, Z.; Webster, T. F. Helsingor statement on poly- and perfluorinated alkyl substances (PFASs). *Chemosphere* **2014,** *114*, 337-339.
8. ECHA European Chemicals Agency Candidate List of Substances of Very High Concern for Authorisation. https://echa.europa.eu/candidate-list-table (02.05.2019),
9. EPA, *2010/2015 PFOA Stewardship Program*. U.S. Environmental Protection Agency: Washington, D.C., USA, **2006**.
10. OECD, *Risk Reduction Approaches for PFASs; Publications Series on Risk Management No. 29*. Organisation for Economic Co-operation and Development: Paris, France, **2015**.
11. *3M Letter to US EPA. Re phase-out plan for POSF-based products (2260600). US EPA Admin Record. 2000;226:1–11*. **2000**.
12. Wang, Z.; Cousins, I. T.; Scheringer, M.; Hungerbühler, K. Fluorinated alternatives to long-chain perfluoroalkyl carboxylic acids (PFCAs), perfluoroalkane sulfonic acids (PFSAs) and their potential precursors. *Environ. Int.* **2013,** *60*, 242-248.
13. Shi, Y.; Vestergren, R.; Zhou, Z.; Song, X.; Xu, L.; Liang, Y.; Cai, Y. Tissue Distribution and Whole Body Burden of the Chlorinated Polyfluoroalkyl Ether Sulfonic Acid F-53B in Crucian Carp (Carassius carassius): Evidence for a Highly Bioaccumulative Contaminant of Emerging Concern. *Environ. Sci. Technol.* **2015,** *49*, (24), 14156-65.
14. Escher, B. I.; Sigg, L., *Chemical Speciation of Organics and of Metals at Biological Interphases. In: v.Leeuwen, H.P., Köster, W. (Eds.), Physicochemical Kinetics and Transport at Biointerfaces. John Wiley & Sons, Ltd, Chichester, UK, pp. 205– 269.* 2004.
15. Smejtek, P.; Wang, S. Distribution of Hydrophobic Ionizable Xenobiotics between Water and Lipid Membranes: Pentachlorophenol and Pentachlorophenate. A Comparison with Octanol-Water Partition. *Arch. Environ. Contam. Toxicol.* **1993,** *25*, 394−404.
16. Avdeef, A.; Box, K. J.; Comer, J. E. A.; Hibbert, C.; Tam, K. Y. pH-Metric logP 10. Determination of Liposomal Membrane-Water Partition Coefficients of Ionizable Drugs. *Pharm. Res.* **1998,** *15*, (2), 209-215.
17. Escher, B. I.; Snozzi, M.; Schwarzenbach, R. P. Uptake,Speciation, and Uncoupling Activity of Substituted Phenols in Energy Transducing Membranes. *Environ. Sci. Technol.* **1996,** *30*, 3071−3079.
18. Perez, F.; Nadal, M.; Navarro-Ortega, A.; Fabrega, F.; Domingo, J. L.; Barcelo, D.; Farre, M. Accumulation of perfluoroalkyl substances in human tissues. *Environ. Int.* **2013,** *59*, 354-362.

19. Maestri, L.; Negri, S.; Ferrari, M.; Ghittori, S.; Fabris, F.; Danesino, P.; Imbriani, M. Determination of perfluorooctanoic acid and perfluorooctanesulfonate in human tissues by liquid chromatography/single quadrupole mass spectrometry. *Rapid Commun. Mass Spectrom.* **2006,** *20*, (18), 2728-2734.
20. Olsen, G. W.; Logan, P. W.; Hansen, K. J.; Simpson, C. A.; Burris, J. M.; Burlew, M. M.; Vorarath, P. P.; Venkateswarlu, P.; Schumpert, J. C.; Mandel, J. H. An Occupational Exposure Assessment of a Perfluorooctanesulfonyl Fluoride Production Site: Biomonitoring. *AIHA Journal* **2003,** *64*, (5), 651-659.
21. Kärrman, A.; Domingo, J. L.; Llebaria, X.; Nadal, M.; Bigas, E.; van Bavel, B.; Lindström, G. Biomonitoring perfluorinated compounds in Catalonia, Spain: concentrations and trends in human liver and milk samples. *Environ. Sci. Pollut. Res. Int.* **2010,** *17*, (3), 750-758.
22. Armitage, J. M.; Arnot, J. A.; Wania, F. Potential role of phospholipids in determining the internal tissue distribution of perfluoroalkyl acids in biota. *Environ. Sci. Technol.* **2012,** *46*, (22), 12285-12286.
23. Luebker, D. J.; Hansen, K. J.; Bass, N. M.; Butenhoff, J. L.; Seacat, A. M. Interactions of flurochemicals with rat liver fatty acid-binding protein. *Toxicology* **2002,** *176*, (3), 175-185.
24. Jones, P. D.; Hu, W.; De Coen, W.; Newsted, J. L.; Giesy, J. P. Binding of Perfluorinated Fatty Acids to Serum Proteins. *Environ. Toxicol. Chem.* **2003,** *22*, (11), 2639–2649.
25. Han, X.; Hinderliter, P. M.; Snow, T. A.; Jepson, G. W. Binding of perfluorooctanoic acid to rat liver-form and kidney-form alpha2u-globulins. *Drug Chem. Toxicol.* **2004,** *27*, (4), 341-360.
26. Han, X.; Snow, T. A.; Kemper, R. A.; Jepson, G. W. Binding of perfluorooctanoic acid to rat and human plasma proteins. *Chem. Res. Toxicol.* **2003,** *16*, (6), 775-81.
27. Allendorf, F.; Berger, U.; Goss, K.-U.; Ulrich, N. Partition coefficients of four perfluoroalkyl acid alternatives between bovine serum albumin (BSA) and water in comparison to ten classical perfluoroalkyl acids. *Environ. Sci.: Processes Impacts* **2019,** *21*, 1852-1863
28. Bischel, H. N.; MacManus-Spencer, L. A.; Zhang, C.; Luthy, R. G. Strong associations of short-chain perfluoroalkyl acids with serum albumin and investigation of binding mechanisms. *Environ. Toxicol. Chem.* **2011,** *30*, (11), 2423-2430.
29. Chen, Y. M.; Guo, L. H. Fluorescence study on site-specific binding of perfluoroalkyl acids to human serum albumin. *Arch. Toxicol.* **2009,** *83*, (3), 255-261.
30. MacManus-Spencer, L. A.; Tse, M. L.; Hebert, P. C.; Bischel, H. N.; Luthy, R. G. Binding of perfluorocarboxylates to serum albumin: a comparison of analytical methods. *Anal. Chem.* **2010,** *82*, (3), 974-981.
31. Messina, P.; Prieto, G.; Dodero, V.; Ruso, J. M.; Schulz, P.; Sarmiento, F. Ultraviolet-circular dichroism spectroscopy and potentiometric study of the interaction between human serum albumin and sodium perfluorooctanoate. *Biopolymers* **2005,** *79*, (6), 300-309.
32. Kerstner-Wood, C.; Coward, L.; Gorman, G. Protein binding of perfluorohexane sulfonate, perfluoroooctane sulfonate and perfluorooctanoate to plasma (human, rat, and monkey), and various human-derived plasma protein fractions. *Southern Research Institute, Study ID 9921.7.* **2003**.
33. Zhang, L.; Ren, X. M.; Guo, L. H. Structure-based investigation on the interaction of perfluorinated compounds with human liver fatty acid binding protein. *Environ. Sci. Technol.* **2013,** *47*, (19), 11293-11301.
34. Sheng, N.; Li, J.; Liu, H.; Zhang, A.; Dai, J. Interaction of perfluoroalkyl acids with human liver fatty acid-binding protein. *Arch. Toxicol.* **2016,** *90*, (1), 217-227.
35. Inoue, T.; Iwanaga, T.; Fukushima, K.; Shimozawa, R. Effect of sodium octanoate and sodium perfluorooctanoate on gel-to-liquid-crystalline phase transition of dipalmitoylphosphatidylcholine vesicle membrane. *Chem. Phys. Lipids* **1988,** *46*, 25-30.
36. Lehmler, H. J.; Bummer, P. M. Mixing of perfluorinated carboxylic acids with dipalmitoylphosphatidylcholine. *Biochim. Biophys. Acta* **2004,** *1664*, (2), 141-149.
37. Lehmler, H. J.; Xie, W.; Bothun, G. D.; Bummer, P. M.; Knutson, B. L. Mixing of perfluorooctanesulfonic acid (PFOS) potassium salt with dipalmitoyl phosphatidylcholine (DPPC). *Colloids Surf. B Biointerfaces* **2006,** *51*, (1), 25-29.

38. Xie, W.; Ludewig, G.; Wang, K.; Lehmler, H. J. Model and cell membrane partitioning of perfluorooctanesulfonate is independent of the lipid chain length. *Colloids Surf. B Biointerfaces* **2010,** *76*, (1), 128-136.
39. Xie, W.; Bothun, G. D.; Lehmler, H. J. Partitioning of perfluorooctanoate into phosphatidylcholine bilayers is chain length-independent. *Chem. Phys. Lipids* **2010,** *163*, (3), 300-308.
40. Nouhi, S.; Ahrens, L.; Campos Pereira, H.; Hughes, A. V.; Campana, M.; Gutfreund, P.; Palsson, G. K.; Vorobiev, A.; Hellsing, M. S. Interactions of perfluoroalkyl substances with a phospholipid bilayer studied by neutron reflectometry. *J. Colloid Interface Sci.* **2018,** *511*, 474-481.
41. Fitzgerald, N. J. M.; Wargenau, A.; Sorenson, C.; Pedersen, J.; Tufenkji, N.; Novak, P. J.; Simcik, M. F. Partitioning and Accumulation of Perfluoroalkyl Substances in Model Lipid Bilayers and Bacteria. *Environ. Sci. Technol.* **2018,** *52*, (18), 10433-10440.
42. Sanchez Garcia, D.; Sjödin, M.; Hellstrandh, M.; Norinder, U.; Nikiforova, V.; Lindberg, J.; Wincent, E.; Bergman, A.; Cotgreave, I.; Munic Kos, V. Cellular accumulation and lipid binding of perfluorinated alkylated substances (PFASs) - A comparison with lysosomotropic drugs. *Chem. Biol. Interact.* **2018,** *281*, 1-10.
43. Droge, S. T. J. Membrane-water partition coefficients to aid risk assessment of perfluoroalkyl anions and alkyl sulfates. *Environ. Sci. Technol.* **2018,** *53*, 760−770.
44. Schwarzenbach, R. P.; Escher, B. I. Partitioning of Substituted Phenols in Liposome-Water, Biomembrane-Water, and Octanol-Water Systems. *Environ. Sci. Technol.* **1996,** *30*, 260-270.
45. Escher, B. I.; Abagyanc, R.; Embry, M.; Klüver, N.; Redmane, A. D.; Zarfl, C.; Parkerton, T. F. Recommendations For Improving Methods And Models For Aquatic Hazard Assessment Of Ionizable Organic Chemicals. *Environ. Toxicol. Chem.* **2020,** *39*, (2), 269-286.
46. Baumer, A.; Bittermann, K.; Klüver, N.; Escher, B. I. Baseline toxicity and ion-trapping models to describe the pH-dependence of bacterial toxicity of pharmaceuticals. *Environ. Sci.: Processes Impacts* **2017,** *19*, (7), 901-916.
47. EPA, *Health Effects Document for Perfluorooctane Sulfonate (PFOS)*. **2014**.
48. EPA, *Health Effects Document for Perfluorooctanoic acid (PFOA)*. **2016**.
49. Watson, H. Biological membranes. *Essays Biochem.* **2015,** *59*, 43-69.
50. Goss, K. U. The pKa Values of PFOA and Other Highly Fluorinated Carboxylic Acids. *Environ. Sci. Technol.* **2008,** *42*, 456–458.
51. Vierke, L.; Berger, U.; Cousins, I. T. Estimation of the acid dissociation constant of perfluoroalkyl carboxylic acids through an experimental investigation of their water-to-air transport. *Environ. Sci. Technol.* **2013,** *47*, (19), 11032-11039.
52. Han, X.; Nabb, D. L.; Russell, M. H.; Kennedy, G. L.; Rickard, R. W. Renal elimination of perfluorocarboxylates (PFCAs). *Chem. Res. Toxicol.* **2012,** *25*, (1), 35-46.
53. Yang, C. H.; Glover, K. P.; Han, X. Organic anion transporting polypeptide (Oatp) 1a1-mediated perfluorooctanoate transport and evidence for a renal reabsorption mechanism of Oatp1a1 in renal elimination of perfluorocarboxylates in rats. *Toxicol. Lett.* **2009,** *190*, (2), 163-171.
54. Yang, C. H.; Glover, K. P.; Han, X. Characterization of cellular uptake of perfluorooctanoate via organic anion-transporting polypeptide 1A2, organic anion transporter 4, and urate transporter 1 for their potential roles in mediating human renal reabsorption of perfluorocarboxylates. *Toxicol. Sci.* **2010,** *117*, (2), 294-302.
55. Weaver, Y. M.; Ehresman, D. J.; Butenhoff, J. L.; Hagenbuch, B. Roles of rat renal organic anion transporters in transporting perfluorinated carboxylates with different chain lengths. *Toxicol. Sci.* **2010,** *113*, (2), 305-314.
56. Nakagawa, H.; Hirata, T.; Terada, T.; Jutabha, P.; Miura, D.; Harada, K. H.; Inoue, K.; Anzai, N.; Endou, H.; Inui, K. Roles of Organic Anion Transporters in the Renal Excretion of Perfluorooctanoic Acid. *Basic Clin. Pharmacol. Toxicol.* **2008,** *103*, 1–8.

57. Katakura, M.; Kudo, N.; Tsuda, T.; Hibino, Y.; Mitsumoto, A.; Kawashima, Y. Rat Organic Anion Transporter 3 and Organic Anion Transporting Polypeptide 1 Mediate Perfluorooctanoic Acid Transport. *J. Health Sci.* **2007,** *53*, (1), 77-83.
58. Zhao, W.; Zitzow, J. D.; Ehresman, D. J.; Chang, S. C.; Butenhoff, J. L.; Forster, J.; Hagenbuch, B. Na+/Taurocholate Cotransporting Polypeptide and Apical Sodium-Dependent Bile Acid Transporter Are Involved in the Disposition of Perfluoroalkyl Sulfonates in Humans and Rats. *Toxicol. Sci.* **2015,** *146*, (2), 363-373.
59. Zhao, W.; Zitzow, J. D.; Weaver, Y.; Ehresman, D. J.; Chang, S. C.; Butenhoff, J. L.; Hagenbuch, B. Organic Anion Transporting Polypeptides Contribute to the Disposition of Perfluoroalkyl Acids in Humans and Rats. *Toxicol. Sci.* **2017,** *156*, (1), 84-95.
60. Han, X.; Yang, C. H.; Snajdr, S. I.; Nabb, D. L.; Mingoia, R. T. Uptake of perfluorooctanoate in freshly isolated hepatocytes from male and female rats. *Toxicol. Lett.* **2008,** *181*, (2), 81-86.
61. Kimura, O.; Fujii, Y.; Haraguchi, K.; Kato, Y.; Ohta, C.; Koga, N.; Endo, T. Uptake of perfluorooctanoic acid by Caco-2 cells: Involvement of organic anion transporting polypeptides. *Toxicol. Lett.* **2017,** *277*, 18-23.
62. Kudo, N.; Katakura, M.; Sato, Y.; Kawashima, Y. Sex hormone-regulated renal transport of perfluorooctanoic acid. *Chem.-Biol. Interact.* **2002,** *139*, (3), 301-316.
63. Ebert, A.; Hannesschlaeger, C.; Goss, K. U.; Pohl, P. Passive Permeability of Planar Lipid Bilayers to Organic Anions. *Biophys. J* **2018,** *115*, (10), 1931-1941.
64. Goss, K. U.; Bittermann, K.; Henneberger, L.; Linden, L. Equilibrium biopartitioning of organic anions - A case study for humans and fish. *Chemosphere* **2018,** *199*, 174-181.
65. Kaiser, S. M.; Escher, B. I. The Evaluation of Lip-Wat Partitioning of 8 Hydroxyquinolines and their copper complexes. *Environ. Sci. Technol.* **2006,** *40*, 1784-1791.
66. New, R. R. C., Ed., *Liposomes - a practical approach*. Oxford University Press: New York, USA, 1990.
67. Bittermann, K.; Spycher, S.; Endo, S.; Pohler, L.; Huniar, U.; Goss, K. U.; Klamt, A. Prediction of Phospholipid-Water Partition Coefficients of Ionic Organic Chemicals Using the Mechanistic Model COSMOmic. *J. Phys. Chem. B* **2014,** *118*, (51), 14833-14842.
68. Escher, B. I.; Schwarzenbach, R. P. Evaluation of Liposome-Water Partitioning of Organic Acids and Bases. 1. Development of a Sorption Model. *Environ. Sci. Technol.* **2000,** *34*, 3954-3961.
69. Huang, X. L.; Zhang, J. Z. Neutral persulfate digestion at sub-boiling temperature in an oven for total dissolved phosphorus determination in natural waters. *Talanta* **2009,** *78*, (3), 1129-1135.
70. Endo, S.; Escher, B. I.; Goss, K. U. Capacities of membrane lipids to accumulate neutral organic chemicals. *Environ. Sci. Technol.* **2011,** *45*, (14), 5912-5921.
71. Henneberger, L.; Goss, K. U.; Endo, S. Equilibrium Sorption of Structurally Diverse Organic Ions to Bovine Serum Albumin. *Environ. Sci. Technol.* **2016,** *50*, (10), 5119-5126.
72. Berger, U.; Glynn, A.; Holmström, K. E.; Berglund, M.; Ankarberg, E. H.; Törnkvist, A. Fish consumption as a source of human exposure to perfluorinated alkyl substances in Sweden - analysis of edible fish from Lake Vättern and the Baltic Sea. *Chemosphere* **2009,** *76*, (6), 799-804.
73. Glynn, A.; Berger, U.; Bignert, A.; Ullah, S.; Aune, M.; Lignell, S.; Darnerud, P. O. Perfluorinated alkyl acids in blood serum from primiparous women in Sweden: serial sampling during pregnancy and nursing, and temporal trends 1996-2010. *Environ. Sci. Technol.* **2012,** *46*, (16), 9071-9.
74. Montal, M.; Mueller, P. Formation of bimolecular membranes from lipid monolayers and a study of their electrical properties. *Proc. Natl. Acad. Sci.* **1972,** *69*, 3561–3566.
75. COSMOthermX (V18 release 1803), COSMOlogic GmbH & Co KG, http://www.cosmologic.de.
76. Ulrich, N.; Endo, S.; Brown, T. N.; Watanabe, N.; Bronner, G.; Abraham, M. H.; Goss, K. U., *UFZ-LSER database v 3.2 [Internet]*. Leipzig, Deutschland, Helmholtz Zentrum für Umweltforschung - UFZ [accessed on 18.11.2019]. Available from http://www.ufz.de/lserd, 2017.

77. TURBOMOLE 4.2.1 (2016), a development of University of Karlsruhe and Forschungszentrum Karlsruhe GmbH, 1989-2007, TURBOMOLE GmbH, since 2007: available from http://www.turbomole.com.
78. COSMOconf (V 4.1), COSMOlogic GmbH & Co KG, http://www.cosmologic.de.
79. Klamt, A. Conductor-like screening model for real solvents: a new approach to the quantitative calculation of solvation phenomena. *J. Phys. Chem.* **1995,** *99*, (7), 2224–2235.
80. Bittermann, K.; Goss, K. U. Predicting apparent passive permeability of Caco-2 and MDCK cell-monolayers: A mechanistic model. *PLoS One* **2017,** *12*, (12), e0190319.
81. JChem for Office, 19.9.0.467 , 2019 ChemAxon (http://www.chemaxon.com).
82. Goss, K. U.; Bronner, G. What Is So Special about the Sorption Behavior of Highly Fluorinated Compounds? *J. Phys. Chem. A* **2006,** *110*, 9518-9522.
83. Dołżonek, J.; Cho, C. W.; Stepnowski, P.; Markiewicz, M.; Thöming, J.; Stolte, S. Membrane partitioning of ionic liquid cations, anions and ion pairs - Estimating the bioconcentration potential of organic ions. *Environ. Pollut.* **2017,** *228*, 378-389.
84. Spycher, S.; Smejtek, P.; Netzeva, T. I.; Escher, B. I. Toward a class-independent quantitative structure-activity relationship model for uncouplers of oxidative phosphorylation. *Chem. Res. Toxicol.* **2008,** *21*, 911–927.
85. Lomize, A. L.; Pogozheva, I. D. Physics-Based Method for Modeling Passive Membrane Permeability and Translocation Pathways of Bioactive Molecules. *J. Chem. Inf. Model* **2019,** *59*, (7), 3198-3213.
86. Boudreau, T. M., Toxicity of Perfluorinated Organic Acids to Selected Freshwater Organisms Under Laboratory and Field Conditions. M.S. Thesis, University of Guelph, Ontario, Canada. In 2002; p 145.
87. Rodea-Palomares, I.; Leganes, F.; Rosal, R.; Fernandez-Pinas, F. Toxicological interactions of perfluorooctane sulfonic acid (PFOS) and perfluorooctanoic acid (PFOA) with selected pollutants. *J. Hazard. Mater.* **2012,** *201-202*, 209-218.
88. Latala, A.; Nedzi, M.; Stepnowski, P. Acute toxicity assessment of perfluorinated carboxylic acids towards the Baltic microalgae. *Environ. Toxicol. Pharmacol.* **2009,** *28*, (2), 167-171.
89. Boström, M. L.; Berglund, O. Influence of pH-dependent aquatic toxicity of ionizable pharmaceuticals on risk assessments over environmental pH ranges. *Water Res.* **2015,** *72*, 154-161.
90. Skolnik, S.; Lin, X.; Wang, J.; Chen, X. H.; He, T.; Zhang, B. Towards prediction of in vivo intestinal absorption using a 96-well Caco-2 assay. *J. Pharm. Sci.* **2010,** *99*, (7), 3246-3265.
91. Gannon, S. A.; Fasano, W. J.; Mawn, M. P.; Nabb, D. L.; Buck, R. C.; Buxton, L. W.; Jepson, G. W.; Frame, S. R. Absorption, distribution, metabolism, excretion, and kinetics of 2,3,3,3-tetrafluoro-2-(heptafluoropropoxy)propanoic acid ammonium salt following a single dose in rat, mouse, and cynomolgus monkey. *Toxicology* **2016,** *340*, 1-9.